29 Mar 2001, 4:00 pm - 6:00 pm

Evaluation Nonlinear Soil Response In Situ

Ellen M. Rathje
University of Texas at Austin, Austin, TX

Ryan D. Phillips
CTL/Thompson, Colorado Springs, CO

Wen-Jong Chang
University of Texas at Austin, Austin, TX

Kenneth H. Stokoe II
University of Texas at Austin, Austin, TX

Evaluating Nonlinear Soil Response In Situ

Ellen M. Rathje
University of Texas at Austin
Austin, TX 78712

Ryan D. Phillips
CTL/Thompson
Colorado Springs, CO

Wen-Jong Chang
University of Texas at Austin
Austin, TX 78712

Kenneth H. Stokoe, II
University of Texas at Austin
Austin, TX 78712

ABSTRACT

Evaluation of nonlinear soil properties is an important concern in geotechnical earthquake engineering. Typically, nonlinear properties are expressed in terms of the nonlinear reduction in shear and constrained moduli with strain and the nonlinear increase in material damping in shear and constrained compression with strain. At this time, there is essentially total dependency on laboratory testing to evaluate nonlinear soil properties. The accuracy and limitations involved in modeling in situ properties with laboratory evaluated properties remains to be studied. In an attempt to evaluate nonlinear soil properties directly in the field, an in situ test method is being developed at the University of Texas that dynamically loads a soil deposit while simultaneously measuring strains, soil properties, and pore water pressures. Initial testing with this method has focused on vertically loading an unsaturated sandy soil, evaluating the magnitude of induced strains, and assessing the variation of constrained modulus (in terms of compression wave velocity, V_P) with effective vertical stress and vertical strain. Preliminary results show that the test method can be used to: (1) evaluate the increase in small-strain V_P with increasing vertical effective stress, (2) induce nonlinear compressional and shear strains, and (3) evaluate the nonlinear reduction in V_P with increasing vertical strain.

INTRODUCTION

Evaluation of nonlinear soil properties (i.e., nonlinear reduction in shear and constrained moduli with strain, nonlinear increase in material damping in shear and constrained compression with strain) is an important concern in geotechnical earthquake engineering. Currently, there is essentially total dependency on laboratory tests to evaluate nonlinear soil properties. In the laboratory, the nonlinear reduction in shear modulus (G) and nonlinear increase in material damping in shear (D_S) with shearing strain (γ) are evaluated over a wide strain range using one or more types of testing equipment. The resulting nonlinear curves are used in site response analyses that model shear wave propagation. When the propagation of compression waves is a concern, the appropriate soil properties are the constrained modulus (M, where $M = \rho V_P^2$, ρ = mass density, V_P = compression wave velocity) and material damping in constrained compression (D_P). It is difficult to measure these properties in the laboratory because it is difficult to maintain a constrained boundary condition in a relatively small soil specimen. Therefore, the nonlinear constrained modulus and constrained material damping are typically assumed to be related to the nonlinear properties in shear, with G and M related by Poisson's ratio, ν, and D_P being some fraction of D_S, on the order of 2/3.

In situ testing offers many advantages over laboratory testing and, hence, typically is the approach of choice when possible. For instance, V_S and V_P are routinely measured in situ using small-strain seismic techniques rather than laboratory testing techniques. However, when the nonlinear variation of G and D_S with γ is required, laboratory testing is normally conducted. Concern always exists about the accuracy with which the in situ properties are represented by laboratory-evaluated values. Differences are known to occur because of sample disturbance, in proper confinement, and non-representative boundary conditions. In situ testing allows these limitations to be overcome. Additionally, in situ evaluation of nonlinear soil properties provides an opportunity to evaluate the accuracy with which current laboratory methods can be used to evaluate nonlinear soil properties.

To begin to measure nonlinear soil properties in situ, a generalized test method is under development at the University of Texas (Phillips 2000). This method involves applying static and dynamic loads at the surface of a soil deposit, and measuring the dynamic response of the soil mass beneath the loaded area using embedded instrumentation. A vibroseis truck is used to apply static and dynamic loads to a large circular footing at the ground surface. A vibroseis truck is an electro-hydraulic shaker used in oil exploration as a seismic source for reflection studies. Instrumentation includes a load cell to measure the loading applied to the footing and embedded velocity transducers (geophones) under and around the loaded area to measure the response of the soil mass. In future testing, pore water pressures will be monitored in saturated soils using piezometers. The result is a load-

controlled dynamic field test that induces soil nonlinearity and generates excess pore water pressures. Initial testing has focused on vertically loading the soil, evaluating the magnitude of induced strains, and assessing the variation of constrained compression wave (P-wave) velocity with effective vertical stress and vertical strain. The research team chose initially to study P-wave velocity rather than shear wave (S-wave) velocity because it is more straightforward to measure P-wave velocity with the vertically oriented vibroseis truck owned by the University of Texas. Evaluating in situ material damping was beyond the scope of this initial test series, but is a priority in future testing.

TEST SETUP

The vibroseis truck owned by the University of Texas was used for an initial test series at a local granular soil quarry in Austin, Texas. A circular, reinforced concrete footing was constructed at the site to transfer load from the hydraulic ram of the vibroseis to the ground surface. The footing was 4 ft (122 cm) in diameter, 1 ft (31 cm) thick, and was embedded approximately 6 in. (15 cm) into the ground. The vibroseis truck was placed over the concrete footing and the loading ram from the truck was lowered onto a steel frame that distributed the load across the footing. A load cell was placed between the ram and steel frame to measure load levels. The vibroseis truck in its loading position is shown in Fig. 1.

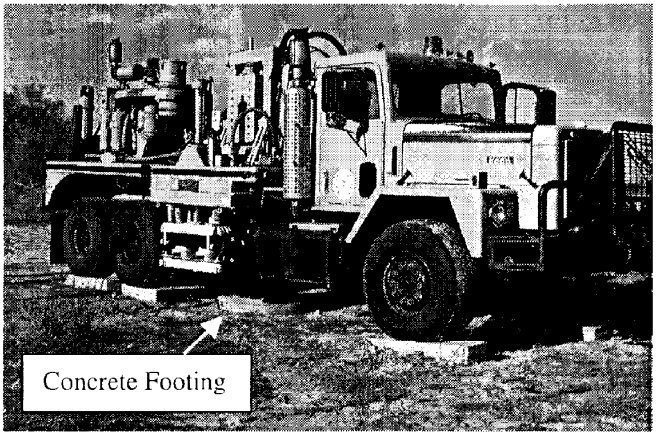

Fig. 1. Vibroseis truck in loading position.

Before the concrete footing was constructed, 11 geophones were embedded at various locations and depths below the ground surface (Fig. 2). These geophones were encased in acrylic cases to protect the instrumentation and to allow them to be oriented accurately in the ground. Three vertically oriented geophones were placed in a vertical array beneath the center of the footing (V1, V2, and V3 in Fig. 2). Eight geophones were placed within approximately one radius from the edge of the circular footing. These eight geophones were placed in four cases, each case containing a horizontal geophone (oriented radially) and a vertical geophone. The four, two-component cases were installed at two radial distances and at two depths, to form a 2 ft by 2 ft (61 cm by 61 cm) square element outside the radius of the footing. The vertical geophone array beneath the center of the footing was used to study constrained compression wave propagation. The array of two-dimensional geophones was used to evaluate shear strains within the square element.

The soil at the test site is poorly graded sand (SP) with 3% finer than the #200 sieve. The upper 6 in. (15 cm) of the soil is cemented crust. The groundwater table is at a depth of about 5 ft (1.5 m). Between the crust and the groundwater table, the soil shows a zone of capillarity, where the water content varies from about 3% to 7%. Downhole and crosshole seismic testing (Chen 2000) indicate an initial compression wave velocity of about 875 ft/s (267 m/s) and an initial shear wave velocity of 600 ft/s (183 m/s) in the sand between 0.5 ft and 4 ft (15 cm and 1.22 m).

The initial test series was conducted over a two-day period, during which multiple loading frequencies and loading levels were applied. For each test, a static load was applied to the footing followed by a sinusoidal dynamic load centered about the static load. Static loads varied from approximately 6 to 24 kips (26.7 to 106.8 kN) and dynamic loads varied from approximately 2 to 8 kips (8.9 to 35.6 kN). Initial difficulties with load control caused the measured loads to differ from the desired loads. At each static and dynamic load level combination, loads were applied at frequencies between 10 Hz and 100 Hz. However, the vibroseis truck had difficulty producing a clean, sinusoidal signal at frequencies below 40 Hz and above 70 Hz. Therefore, only data from 40 Hz and 70 Hz tests are presented.

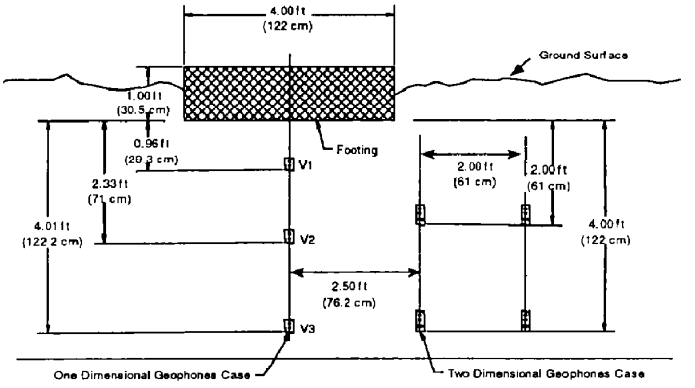

Fig. 2. Embedded instrumentation locations.

DATA ANALYSIS

The goals of the initial test series were to load the soil at several different load levels, evaluate the change in P-wave velocity with increasing vertical effective stress, and evaluate the change in P-wave velocity, and hence M , with increasing vertical strain. Towards that end, the effective vertical stress under the applied static load, the P-wave velocity, and the

vertical strain-time history were calculated between cases V1-V2 and V2-V3 for each test.

To estimate the vertical effective stress at the midpoint between the vertical geophones, the initial vertical stress was calculated assuming a total unit weight of 125 pcf and negative pore water pressures due to static capillary stresses above the ground water table. For a rigid footing on sand, limited data indicates that the stress distribution at the bottom of the footing is approximately parabolic, with the maximum pressure equal to twice the surface pressure (Farber 1933) and the pressure at the edges of the footing equal to zero. Assuming this stress distribution at the ground surface, the pressure distribution was modeled with several circular uniform loads of varying radii. Superimposing these loaded areas resulted in an approximate parabolic stress distribution. The elastic solution for each circular uniform load on an isotropic, homogeneous, weightless, elastic half-space was summed to estimate the increase in vertical stress at points below the footing. This stress was added to the initial vertical effective stress to calculate the vertical effective stress at points centered between cases V1-V2 and V2-V3.

The analytical solution for a vertically vibrating footing on an elastic halfspace can be used to understand wave propagation beneath the footing. A vertically vibrating footing generates compression, shear, and surface waves in the underlying material. Beneath the center of the footing the amplitudes of the shear and surface waves are zero, and motion is generated only by the compression wave (Richart et al. 1970). Therefore, vertical geophones below the center of the footing can be used to evaluate the travel time of P-waves in the soil. Essentially, the phase difference between pairs of geophones measured during sinusoidal loading represents the travel time of a wave between the geophones. This travel time is calculated using spectral analysis of the time records (i.e., cross power spectrum, as described by Stokoe et al. 1994) between the vertical geophones embedded under the center of the footing. With the distance between the geophones known, the velocity of the P-wave between these geophones was calculated using the travel time.

Vertical strains (ε_a) were derived from the recorded velocity-time histories below the footing. Displacement-time histories were calculated by numerical integration of the velocity-time histories using the trapezoidal method. The relative displacement between vertical geophones and the distance between geophones were used to calculate the average vertical strain between the geophones, and peak strains were used for all relationships regarding strain.

To estimate the shear strains within the square element located outside the radius of the footing, again displacement-time histories were derived from the recorded velocity-time histories. However, the finite element formulation was used to calculate the shear strain at the center of the element. A 4-node, isoparametric element, which assumes a linear variation of displacement between finite element nodes, was incorporated to calculate strains within the square element.

RESULTS FROM LINEAR AND NONLINEAR MEASUREMENTS

As noted earlier, analyses were performed on data from tests at frequencies of 40 Hz and 70 Hz. The load combinations for these frequencies are shown in Table 1. The desired and measured loads in Table 1 are not the same because of inaccurate load control during testing. In future testing, better load control will be obtained using a dynamic signal analyzer to operate the vibroseis truck.

Table 1. Static and dynamic load combinations.

	Static Load (kips)		**Dynamic Load (kips)**	
Freq (Hz)	Desired	Measured	Desired	Measured
40	6	6.13	2	1.63
	6	5.95	4	3.45
	12	11.30	2	2.30
	12	13.00	4	2.25
	12	13.88	8	5.88
	24	22.75	2	2.75
	24	24.88	4	2.63
	24	25.00	8	6.50
	12	11.50	2	1.90
70	6	--*	2	--*
	6	6.88	4	2.88
	12	12.00	2	1.75
	12	13.00	4	2.75
	12	14.00	8	5.50
	24	23.68	2	2.13
	24	24.75	4	3.00
	24	25.13	8	6.88
	12	11.63	2	2.13

* Data acquisition malfunctioned.

The P-wave velocities evaluated from tests incorporating a 24-kip static load were significantly smaller than those from tests at static loads of 6- and 12-kips (at the same strain level), indicating that a permanent change in the soil properties occurred upon application of the 24-kip load. Additionally, the load combination of 12-kip static ± 2-kip dynamic was repeated after the 24-kip loadings, and indicated a smaller V_P than the original 12-kip ± 2-kip loading (743 f/s vs. 1396 f/s). These changes are most likely due to a state of local shear failure and associated straining beneath the footing. Consequently, only data from the 6- and 12-kip static loads are presented here.

Variation of V_P with Vertical Effective Stress

The effective stresses in the direction of wave propagation and particle motion have a significant influence on measured body wave velocities of soil (Lee 1993). For a vertically propagating compression wave, the directions of wave propagation and particle motion are vertical. Therefore, the vertical effective stress is the only relevant stress that affects P-wave velocity in these tests. Measured wave velocities at

relatively small strains ($\varepsilon_a < 0.005$ %) were used to investigate this relationship in situ.

Compression wave velocities measured with the shallow receivers (V1-V2) are presented in Fig. 3. Stokoe et al. (1995) presented a power law relationship between P-wave velocity and effective stress as:

$$V_P = C\,(\sigma'_a)^m \qquad (1)$$

where C is a material constant, σ'_a is the effective stress in the direction of wave propagation, and m is the slope of the log V_P -log σ'_a relationship. This power law relationship is shown in Fig. 3. The relationship is fit through the downhole seismic data, using a value of $m = 0.25$. This value of the parameter m in Fig. 3 fits the average data well.

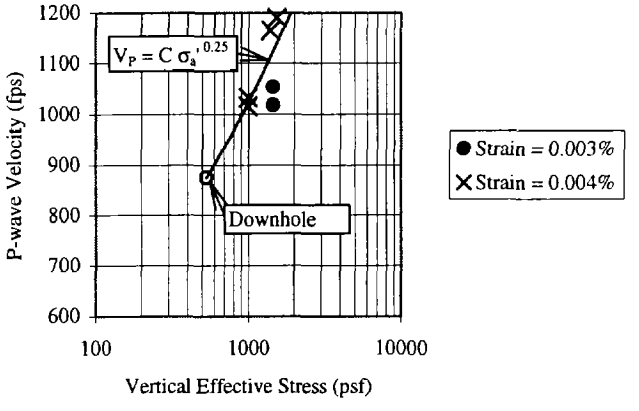

Fig. 3. V_P vs. effective stress for receivers V1-V2.

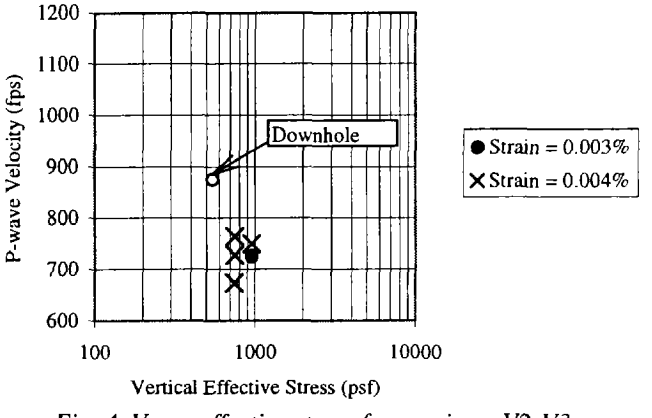

Fig. 4. V_P vs. effective stress for receivers V2-V3.

The V_P data for receivers V2-V3 are shown in Fig. 4, without the power law relationship. This relationship was not added because it does not fit the data from the deeper receivers. In fact, the deeper receivers do not show an increase in P-wave velocity with increasing vertical effective stress, contrary to expected performance. The discrepancy may be due to problems in determining the actual state of stress below the footing. If arching occurred upon backfilling of the geophone borehole, the arch conceivably could redistribute the local stresses in the soil causing the vertical effective stress to be different than the calculated values. Further testing is underway to investigate this discrepancy.

Variation of V_P and M with Vertical Strain

The effect of vertical strain on P-wave velocity is shown in Fig. 5 for receivers V1-V2. To combine data from different static load levels, a stress correction was incorporated using the power law relationship presented in Equation (1). The P-wave velocity was stress-corrected by the factor $(\sigma_a')^m$, using the calculated vertical effective stress and $m = 0.25$. This stress correction allows data to be compared on one graph, regardless of the in situ static effective stress. For comparison, the stress-corrected downhole P-wave velocity is shown at a strain level of 0.0001%. The strain level of 0.0001% was selected to represent the very small strains generated in field downhole seismic tests. The P-wave velocities measured between V1-V2 at different loads levels clearly exhibit nonlinear behavior in Fig. 5. The general trend is a reduction in stress-corrected V_P with increasing vertical strain. Typical hyperbolic functions fit through the downhole data that bound the vibroseis data are shown in Fig. 5 for comparison.

Stress-corrected V_P vs. vertical strain data for receivers V2-V3 are presented in Fig. 6. There is a general trend for a decrease in stress-corrected V_P with increasing vertical strain, but more scatter is observed in this data set. Because the raw V_P data from receivers V2-V3 do not indicate an increase in V_P with the estimated vertical effective stress (Fig. 4), the stress correction does not reduce the scatter. To avoid relying on stress corrections to study the variation of V_P with strain, future testing will incorporate a larger range of dynamic load levels for each static load level.

The V_P data previously presented can be easily converted into constrained modulus (M) using:

$$M = \rho\, V_P^2 \qquad (2)$$

However, the constrained modulus also must be stress corrected. Substituting Equation (1) into Equation (2) for V_P, the relationship between M and vertical effective stress is:

$$M = \rho\, C^2\, (\sigma'_a)^{2m} \qquad (3)$$

This expression indicates that the constrained modulus should be stress corrected using a stress exponent of $2m$ rather than m. Stress-correcting the constrained modulus data using Equation (3) and normalizing this data by the maximum, small strain, stress-corrected constrained modulus allows an M/M_{max} curve to be developed. The stress-corrected value of constrained modulus from downhole seismic testing is termed M_{max} and is used to represent the maximum value of the constrained modulus at small strains.

Because normalized constrained modulus curves have never been measured before in geotechnical earthquake engineering, it is difficult to evaluate the validity of the field test results.

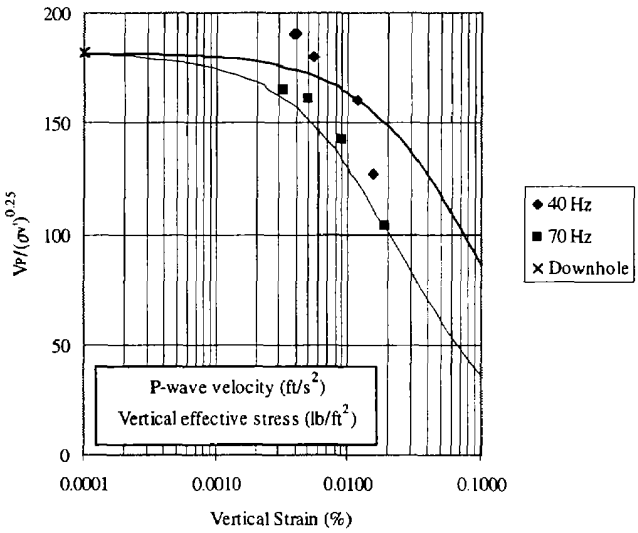

Fig. 5. Stress-corrected V_P vs. vertical strain for receivers V1-V2.

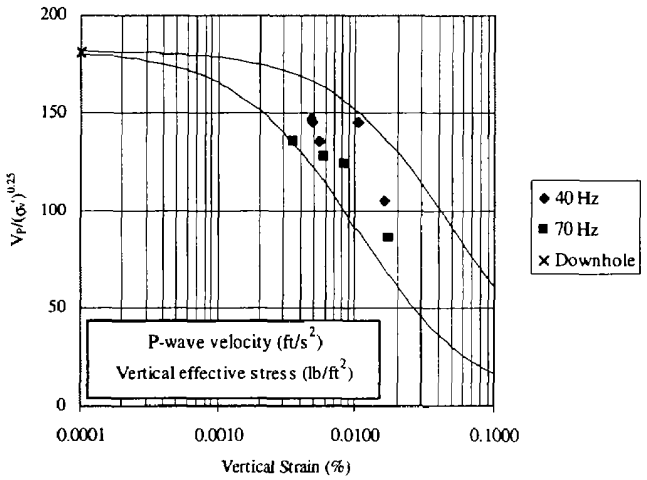

Fig. 6. Stress-corrected V_P vs. vertical strain for receivers V2-V3.

However, a typical normalized shear modulus reduction curve can be transformed into vertical strain and compared to the constrained modulus data. This transformation uses Mohr's circle for strain to relate shear strain to equivalent values of vertical strain under constrained conditions (Fig. 7). Because a constrained wave does not induce strain in the direction perpendicular to the direction of wave propagation, there are no horizontal strains in this test. Shear strains are also zero on the vertical and horizontal planes because the shear wave amplitude is zero. Consequently, the vertical strain is equal to the maximum shear strain (Fig. 7).

A normalized shear modulus curve is plotted with the normalized constrained modulus data in Fig. 8 for receivers V1-V2 and in Fig. 9 for receivers V2-V3. The normalized shear modulus curve was obtained using a hyperbolic model:

$$G/G_{max} = 1/(1+(\gamma/\gamma_r)) \quad (4)$$

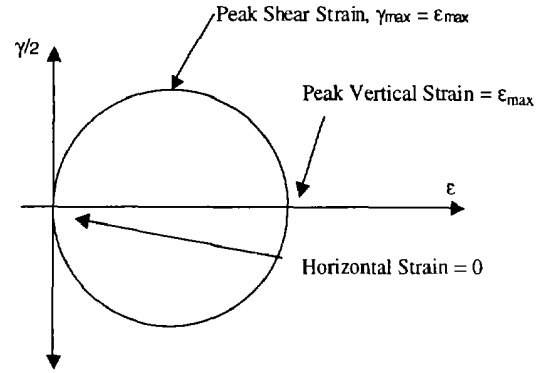

Fig. 7. Mohr's circle of strain for constrained compression wave.

where γ_r = reference strain. A reference strain of 0.02% was used, which is representative of shallow sands (Darendeli 2001). The normalized shear modulus reduction curve fits the data well for the shallower receivers (Fig. 8), but again the data show more variation for the deeper receivers (Fig. 9). Obviously, these hyperbolic curves do not account for changes in modulus reduction with confining pressure. The low values of the normalized constrained modulus in Fig. 9 are likely due to the unknown state of stress, as discussed previously.

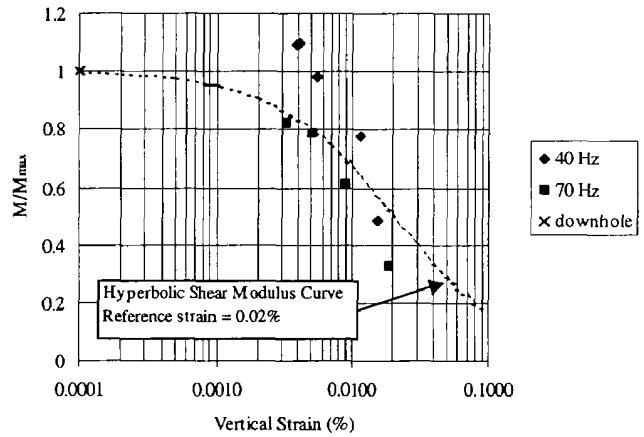

Fig. 8. Normalized constrained modulus data (V1-V2).

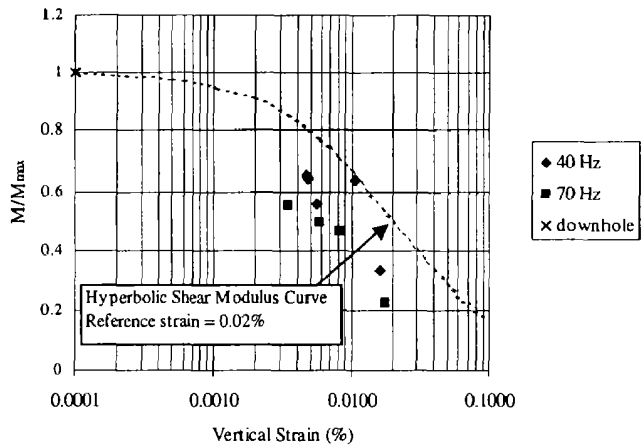

Fig. 9. Normalized constrained modulus data (V2-V3).

Shear Strains Evaluated from Testing

Because the goals of future testing with the vibroseis include inducing and measuring excess pore water pressures and liquefaction potential in situ, shear strains were evaluated at the center of the square element located outside of the radius of the footing. The location of the square element was based on axisymmetric finite element analyses that indicated that the largest shear strains would be generated in this zone.

The 4-node, isoparametric finite element formulation was used to evaluate the shear strain-time history at the center of the square element. Horizontal and vertical displacement-time histories, computed from the recorded velocity-time histories at the nodes, were used in the finite element calculation. The shear strains calculated from the field tests ranged from 0.002 % to 0.012 %. These shear strain levels are around the threshold value for pore pressure generation, indicating that excess pore water pressures can be induced in saturated soils with the testing method under development.

CONCLUSIONS

Evaluation of the variation in small-strain P-wave velocity with σ_v' and the nonlinear variation in V_P with vertical strain were successfully performed in situ. A vibroseis truck was used to generate a controlled combination of static and dynamic loads that were applied to a foundation at the surface of a sandy soil deposit. Embedded geophone arrays were used to measure the response of the soil to these loads. The relationship between small-strain P-wave velocity and vertical effective stress was studied by measuring P-wave velocities during steady-state dynamic loading under different levels of static loading. An increase in P-wave velocity was observed with increasing static effective stress in most cases. The power law relationship proposed by Stokoe et al. (1995) fit the V_P – log σ_v' data from the shallower receivers (V1-V2) well. For the deeper receivers (V2-V3), the P-wave velocity did not clearly show the expected trend, possibly due to arching in the backfill above the deepest geophone.

The measured values of P-wave velocity and constrained modulus showed a clear reduction in magnitude with increased vertical strain. This reduction was observed at each static load level when the dynamic load was increased, inducing larger dynamic strains. To compare various static loading levels, P-wave velocities were normalized by $(\sigma_v')^{0.25}$. In most cases, this normalization helped reduce the scatter in the data and allowed all levels of effective stress to be compared simultaneously. Normalized constrained modulus (M/M_{max}) data from the field tests compared well with normalized constrained modulus reduction curves developed from typical shear modulus reduction curves. Additionally, significant shear strains were developed within the square element outside the radius of the footing, indicating that excess pore water pressures should be induced during future testing of saturated soils.

The testing procedure and methods of data analysis are still in development, but this initial test series has lead to several important conclusions regarding the design of an in situ testing procedure to measure nonlinear soil properties. With further tests, it should be possible to measure more material properties, such as shear wave velocity and material damping in shear and compression, and draw conclusions about dynamic soil behavior and in situ states of stress for coarse-grained soils. Upon refinement of the testing method, generation of pore water pressures for the purpose of in situ liquefaction evaluation will be possible. Data from test involving the generation of pore water pressure will be extremely useful in understanding liquefaction and refining liquefaction evaluation techniques.

ACKNOWLEDGEMENTS

Financial support was provided by the National Science Foundation under Grant CMS-9875430, by the United States Geological Survey under FY 2000 NEHRP Grant 00HGGR0015, and by a University of Texas Research Grant. This support is gratefully acknowledged.

REFERENCES

Chen, J.-Y. [2000] M.S. Thesis, University of Texas at Austin, in progress.

Darendeli, M. [2001] Ph.D. Dissertation, University of Texas at Austin, in progress.

Farber. O. [1933] *Pressure Distribution under Bases and Stability of Foundations.* Jour. of the Institution of Str. Eng., Vol. XI, No. 3, pp. 116-125.

Lee, N.J. [1993] *Experimental Study of Body Wave Velocities in Sand under Anisotropic Conditions.* Ph.D. Dissertation, University of Texas at Austin.

Phillips, R. D. [2000] "Initial Design and Implementation of an In Situ Test for Measurements of Nonlinear Soil Properties," M.S. Thesis, University of Texas at Austin.

Richart, F.E., J.R. Hall, and R.D. Woods [1970] *Vibration of Soils and Foundations.* Prentice Hall, Englewood Cliffs, NJ.

Stokoe, K.H. II, S.G. Wright, J.A. Bay, and J.M. Roesset [1994] *Characterization of Geotechnical Sites by SASW Method.* 13th Int. Conf. on Soil. Mech. and Fndn Eng., New Delhi, India, pp 146.

Stokoe, K.H. II, S.K. Hwang, J.N. Lee, and R.D. Andrus [1995] Effects of Various Parameters on the Stiffness and Damping of Soils at Small to Medium Strains. Proc., Int. Symp. on Pre-Failure Deformation of Geomaterials, Sapporo, Japan, pp. 785-816.